Electronic Supplementary Information (ESI)

Band Gap Modulation and Nonlinear Optical Properties of Quaternary Tellurates Li_2GeTeO_6

Dan Wang,[a#] Yunxi Zhang,[a#] Qian Liu,[a] Bingbing Zhang,[a] Daqing Yang,[a] and Ying Wang*[a]

[a] *College of Chemistry and Environmental Science, Hebei University, Baoding 071002, China. Email: wangy@hbu.edu.cn.*

[#] *These authors contributed equally to this work.*

Table of contents

1. Experimental section……....S2
2. Table S1. Crystal data and structure refinements……...S5
3. Table S2. Atomic coordinates and equivalent isotropic displacement parameters……S6
4. Table S3. Bond lengths [Å] and angles [deg]……S7
5. Table S4. Comparison of structure and optical properties of NLO active-quaternary tellurates.. ……..S9
6. Figure S1. Structural comparison of Li_2ZrTeO_6, α-Li_2HfTeO_6, Li_2SnTeO_6, and Li_2TiTeO_6..S10
7. Figure S2. The SEM and EDX graph of Li_2GeTeO_6……..……S11
8. Figure S3. The calculated and experimental powder XRD patterns of Li_2GeTeO_6……S12
9. Figure S4. The TG and DSC curves of Li_2GeTeO_6……..S13
10. Figure S5. The IR spectrum of Li_2GeTeO_6……..……S14
11. Figure S6. The bandgap of of Li_2GeTeO_6……S15
12. Figure S7. The PDOS of Li_2GeTeO_6 .....S16
13. Figure S8. SHG density maps of the occupied and unoccupied orbitals in the VH process of Li_2GeTeO_6……...S17
14. Reference…… …S18

Experimental section

Synthesis. All chemicals were used as received. Li_2CO_3 (≥99.0%, aladdin), GeO_2 (99.99%, Hawk), and TeO_2 (99.99%, Hawk) were all used as raw materials. Single crystals of Li_2GeTeO_6 were obtained by using the high-temperature flux method. The mixture of Li_2CO_3, GeO_2, and TeO_2 in a molar ratio of 2.5 : 1 : 4 was fully grounded and placed in an alumina crucible. The crucible was heated to 720 °C in 3 h, and held at this temperature for 12 h. Afterward, the solution was cooled slowly to 500 °C with a rate of 2 °C h^{-1}, and then cooled the room temperature quickly. Colorless crystals of Li_2GeTeO_6 were obtained from the surface of the crucible (yield: about 70% based on Ge).

The polycrystalline powder samples of Li_2GeTeO_6 were prepared via the solid-state reaction method in air. A mixture of Li_2CO_3, TeO_2, and GeO_2 with a stoichiometric ratio was fully ground and loaded into a corundum crucible, heated to 700 °C at a rate of 3 °C min^{-1}, held at this temperature for 48 hours, then heat to 750 °C for 12 h with several intermittent grindings. The chemical reaction process can be expressed as follows: $Li_2CO_3 + GeO_2 + TeO_2 + 1/2\ O_2 = Li_2GeTeO_6 + CO_2$.

Characterization. The single-crystal X-ray diffraction (XRD) data were collected on a Bruker D8 VENTURE dual-wavelength Mo/Cu three-circle diffractometer with a microfocus sealed X-ray tube using mirror optics as monochromator and a Bruker PHOTON III detector. The diffractometer used MoK_α radiation (λ = 0.71073 Å) for data collection. All data were integrated with SAINT program[1] and a multi-scan absorption correction using SADABS[2] was applied. The structure was solved by Intrinsic Phasing methods using SHELXT[3] and refined by full-matrix least-squares methods against F^2 by SHELXL[4], embedding within the *Olex*2 program.[5] Potential higher symmetry was checked by PLATON.[6] Crystal data and refinement details, atomic coordinates, and selected bond distances and angles are listed in Tables S1-S3. Powder XRD data were measured on a Dandong Haoyuan DX-27mini X-ray diffractometer with Cu Kα radiation (λ = 1.54056 Å). The powder XRD pattern was scanned over the 2θ angles range of 10-70°, at a scanning step width of 0.02° and a

fixed counting time of 2 s. The thermal gravimetric (TG) analysis and differential scanning calorimetry (DSC) were studied with a NETZSCH5 instrument under air. The sample was placed in an Al_2O_3 crucible and heated from 30 to 1000 °C with a heating rate of 10 °C·min^{-1}. The infrared spectra were recorded on a Shimadzu IR Affinity-1 Fourier transform infrared spectrometer in the range of 400 - 4000 cm^{-1}. The sample was grounded and mixed with KBr. The UV−Vis−NIR diffuse reflectance spectra were measured at room temperature with a Shimadzu SolidSpec-3600DUV spectrophotometer in the 200-1100 nm wavelength range. The SHG effects of the powder samples were measured by using a modified Kurtz-Perry method[7] with a Q-switched 1064 nm Nd: YAG laser. The samples were ground and divided into fractions according to different particle size ranges: 20-38.5, 38.5-55, 55-80, 80-125, 125-160, 160-200, and 200-250 μm. The same particle-sized KDP samples were used as the standard. The optical damage induced by the laser was tested on crystalline powder pellet samples using a Q-switched 1064 nm Nd: YAG laser (1064 nm, 7 ns, 1 Hz). The pulse energy was changed from 20 to100 mJ and a convex lens was used to adjust the beam diameter. The damaged area can be directly observed under a microscope.

Theoretical Calculations. The electronic structures and optical properties for Li_2GeTeO_6 were calculated by using the CASTEP package.[8] The generalized gradient-approximation (GGA) with Perdew-Burke-Ernzerhof (PBE) functional was adopted to describe the exchange-correlation potential.[9] The norm-conserving pseudopotentials (NCP) were adopted to model the effective interaction between the valence electrons and atom cores.[10] The configurations for diverse electron orbital were Li: $2s^2$, Ge: $4s^24p^2$, Te: $5s^25p^4$, and O: $2s^22p^4$, respectively. The cut off energies and the dense *K*-points in the Brillouin zone were set as 750 eV and 3 × 3 × 2. In addition, a scissors operator was used to correct the underestimation of band gap induced by PBE-GGA. On the basis of the scissor-corrected electron band structure, the second-order NLO coefficients d_{ij} were calculated using the length-gauge formalism at a zero-frequency limit.[11] The static second-order nonlinear susceptibilities can be ascribed to Virtual-Hole (VH) and Virtual-Electron (VE) processes. In addition, to visualize the

contribution of each atom to the SHG response, the SHG-weighted electron density method was adopted.[12, 13]

Table S1. Crystal data and structure refinements for Li_2GeTeO_6.

Compound	**Li_2GeTeO_6**
Formula weight	310.07
Temperature (K)	273(2)
Crystal system	Trigonal
Space group (number)	$R3$ (No. 146)
a (Å)	4.996(3)
b (Å)	4.996(3)
c (Å)	14.335(12)
Volume (Å^3)	309.8(5)
Z	3
ρ_{calc} (g·cm^{-3})	4.985
μ (mm^{-1})	14.272
F(000)	414
2Θ range (deg.)	8.53 to 56.61
Limiting indices	$-6 \le h \le 6$; $-6 \le k \le 6$; $-18 \le l \le 18$
Reflections collected / unique	1414
Independent reflections	353 (R_{int} = 0.0733, R_{sigma} = 0.0629)
Completeness to Θ = 25.242°	100.0 %
Data / restraints / parameters	353/7/32
Goodness-of-fit on F^2	1.085
R_1, wR_2 [$F_o^2 > 2\sigma(F_o^2)$][a]	R_1 = 0.0323; wR_2 = 0.0575
R_1, wR_2 (all data) [a]	R_1 = 0.0424; wR_2 = 0.0598
Largest diff. peak and hole (e·Å^{-3})	1.94/-1.27
Flack parameter	0.23(6)

[a] $R_1 = \Sigma||F_o| - |F_c||/\Sigma|F_o|$ and $wR_2 = [\Sigma w(F_o^2 - F_c^2)^2/ \Sigma w F_o^4]^{1/2}$ for $F_o^2 > 2\sigma(F_o^2)$.

Table S2. Atomic coordinates and equivalent isotropic displacement parameters for Li_2GeTeO_6. U(eq) is defined as one-third of the trace of the orthogonalized U_{ij} tensor.

atom	*x*	*y*	*z*	U(eq)	BVS
Li(1)	0.666667	0.333333	0.635(4)	0.02(2)	0.906
Li(2)	0.333333	0.666667	0.699(4)	0.020(15)	0.909
Ge(1)	0.000000	0.000000	0.50701(15)	0.0071(7)	3.910
Te(1)	0.333333	0.666667	0.49362(15)	0.0110(5)	6.004
O(1)	0.298(5)	0.340(5)	0.575(3)	0.013(6)	1.915
O(2)	0.678(5)	0.708(4)	0.425(2)	0.005(5)	1.995

Table S3. Bond lengths [Å] and angles [degree] for Li_2GeTeO_6.

Atom–Atom	Length [Å]	Atom–Atom–Atom	Angle [°]
Li1–O1	2.05(4)	O1–Li1–O1	103(2)
Li1–O1$^{\#1}$	2.05(4)	O1–Li1–O1	103(2)
Li1–O1$^{\#2}$	2.05(4)	O1–Li1–O1	103(2)
Li1–O2$^{\#3}$	2.35(5)	O1–Li1–O2	156(3)
Li1–O2$^{\#4}$	2.35(5)	O1–Li1–O2	89.3(8)
Li1–O2$^{\#5}$	2.35(5)	O1–Li1–O2	93.4(11)
Li2–O2$^{\#5}$	2.03(3)	O1–Li1–O2	89.3(8)
Li2–O2$^{\#9}$	2.03(3)	O1–Li1–O2	93.4(11)
Li2–O2$^{\#10}$	2.03(3)	O1–Li1–O2	156(3)
Li2–O1	2.37(5)	O2–Li1–O2	69.2(16)
Li2–O1$^{\#11}$	2.37(5)	O1–Li1–O2	93.4(11)
Li2–O1$^{\#12}$	2.37(5)	O1–Li1–O2	156(3)
Ge1–O1$^{\#13}$	1.87(3)	O1–Li1–O2	89.3(8)
Ge1–O1$^{\#14}$	1.87(3)	O2–Li1–O2	69.2(16)
Ge1–O1	1.87(3)	O2–Li1–O2	69.2(16)
Ge1–O2$^{\#15}$	1.93(2)	O2–Li2–O2	103.7(19)
Ge1–O2$^{\#11}$	1.93(2)	O2–Li2–O2	103.7(19)
Ge1–O2$^{\#1}$	1.93(2)	O2–Li2–O2	103.7(19)
Te1–O2$^{\#11}$	1.90(3)	O2–Li2–O1	93.2(10)
Te1–O2$^{\#12}$	1.90(3)	O2–Li2–O1	89.0(8)
Te1–O2	1.90(3)	O2–Li2–O1	156(3)
Te1–O1$^{\#12}$	1.94(2)	O2–Li2–O1	156(3)
Te1–O1$^{\#11}$	1.94(2)	O2–Li2–O1	93.2(10)
Te1–O1	1.94(2)	O2–Li2–O1	89.0(8)
		O1–Li2–O1	69.2(17)
		O2–Li2–O1	89.0(8)
		O2–Li2–O1	156(3)
		O2–Li2–O1	93.2(10)
		O1–Li2–O1	69.2(17)
		O1–Li2–O1	69.2(17)
		O1–Ge1–O1	95.7(12)
		O1–Ge1–O1	95.7(12)
		O1–Ge1–O1	95.7(12)
		O1–Ge1–O2	95.5(4)
		O1–Ge1–O2	82.1(6)
		O1–Ge1–O2	168.8(9)
		O1–Ge1–O2	168.8(9)
		O1–Ge1–O2	95.5(4)

O1–Ge1–O2	82.1(6)
O2–Ge1–O2	87.1(15)
O1–Ge1–O2	82.1(6)
O1–Ge1–O2	168.8(9)
O1–Ge1–O2	95.5(4)
O2–Ge1–O2	87.1(15)
O2–Ge1–O2	87.1(15)
O2–Te1–O2	95.8(11)
O2–Te1–O2	95.8(11)
O2–Te1–O2	95.8(11)
O2–Te1–O1	168.6(9)
O2–Te1–O1	95.5(4)
O2–Te1–O1	81.4(9)
O2–Te1–O1	95.5(4)
O2–Te1–O1	81.4(9)
O2–Te1–O1	168.6(9)
O1–Te1–O1	87.8(15)
O2–Te1–O1	81.4(9)
O2–Te1–O1	168.6(9)
O2–Te1–O1	95.5(4)
O1–Te1–O1	87.8(15)
O1–Te1–O1	87.8(15)

Symmetry transformations used to generate equivalent atoms:

#1: 1-Y, +X-Y, +Z; #2: 1-X+Y, 1-X, +Z; #3: 1.66667-Y, 0.33333+X-Y, 0.33333+Z; #4: -0.33333+X, -0.66667+Y, 0.33333+Z; #5: 0.66667-X+Y, 1.33333-X, 0.33333+Z; #6: 0.66667+X, 0.33333+Y, 0.33333+Z; #7: 1+X, +Y, +Z; #8: +X, -1+Y, +Z; #9: 0.66667-Y, 0.33333+X-Y, 0.33333+Z; #10: -0.33333+X, 0.33333+Y, 0.33333+Z; #11: -X+Y, 1-X, +Z; #12: 1-Y, 1+X-Y, +Z; #13: -1+X, +Y, +Z; #14: +X, 1+Y, +Z; #15: -X+Y, -X, +Z; #16: -Y, +X-Y, +Z; #17: -1+X, -1+Y, +Z; #18: -0.66667+X, -0.33333+Y, -0.33333+Z; #19: 1+X, 1+Y, +Z; #20: 0.33333+X, -0.33333+Y, -0.33333+Z; #21: 0.33333+X, 0.66667+Y, -0.33333+Z;

Table S4. Comparison of structure and optical properties of NLO active-quaternary tellurates.

compounds	space group	octahedral distortion Δd		band gap (eV)	SHG (× KDP)	transparent region (μm)	LDT (MW cm^{-2})
		MO_6	TeO_6				
Li_2TiTeO_6	*Pnn*2	0.20	0.06	3.26	26	0.38-6.72	550
Li_2ZrTeO_6	*R*3	0.12	0.02	4.06	2.5	0.29-7.4	1300
α-Li_2HfTeO_6	*R*3	0.19	0.06	3.98	2.2	0.27-8[#]	1000
Li_2SnTeO_6	*Pnn*2	0.01	0.09	3.26	2.5	0.38-6.86	672
Li_2GeTeO_6[*]	*R*3	0.16	0.13	4.65	1.3	0.24-10[#]	1725

*This work

#Based on polycrystalline samples. It should be noted that the IR cut-off edges is deduced from powder IR spectrum which were not highly precise.

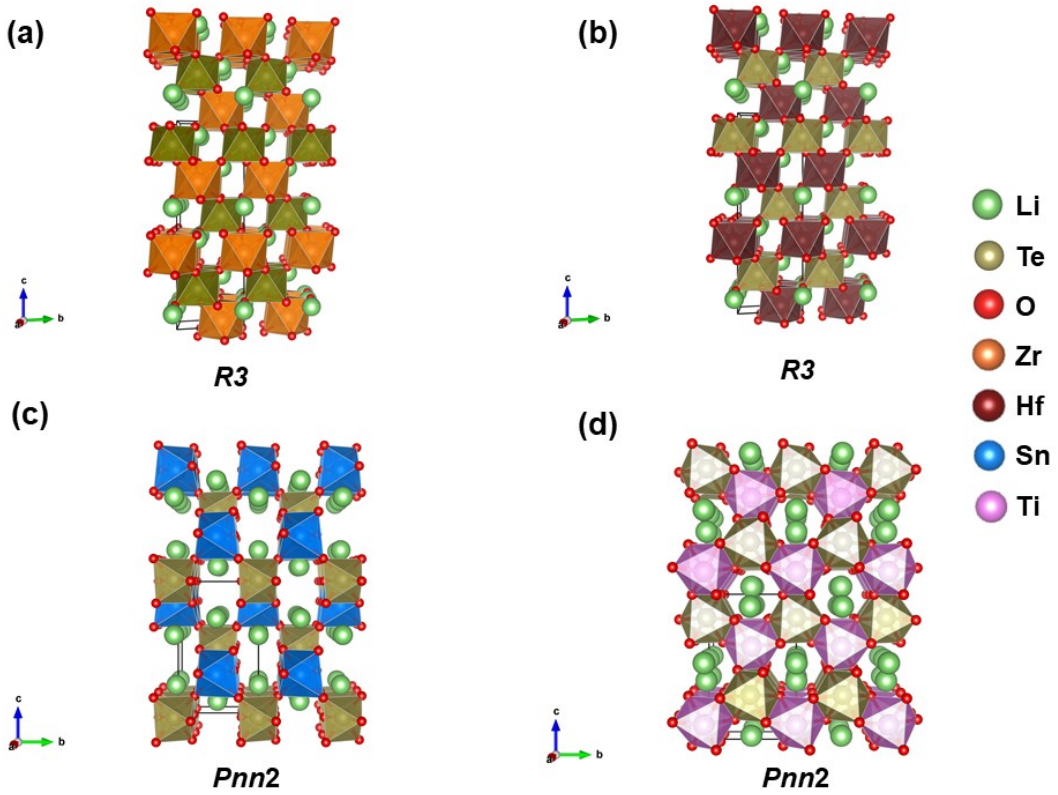

Figure S1. Structural comparison of (a) Li_2ZrTeO_6, (b) α-Li_2HfTeO_6, (c) Li_2SnTeO_6, and (d) Li_2TiTeO_6.

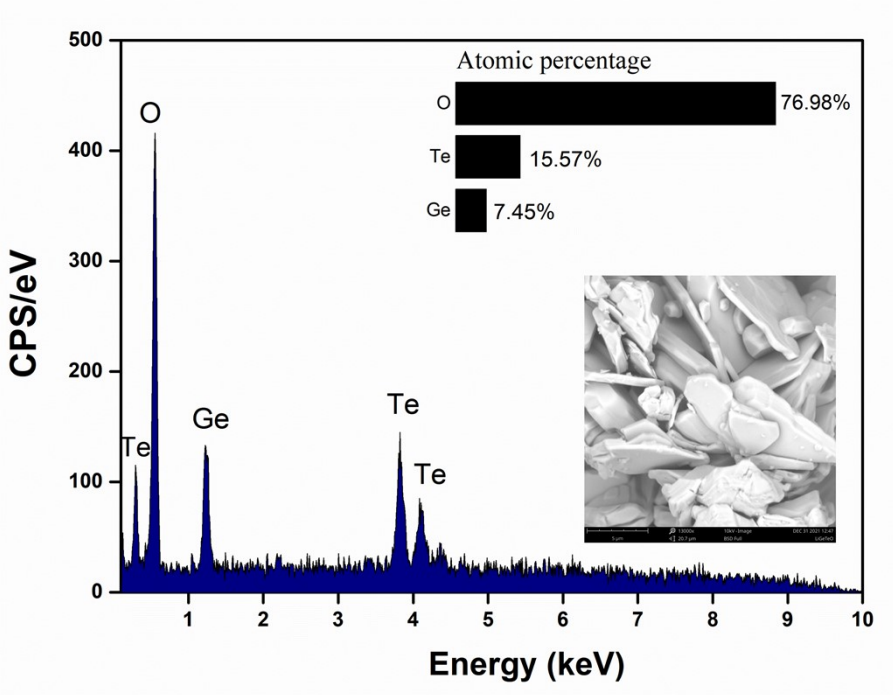

Figure S2. The SEM and EDX of Li_2GeTeO_6 . Noted that the EDX only provides semi-quantitative results, and the Li elements are ignored due to the drawback of EDX analysis.

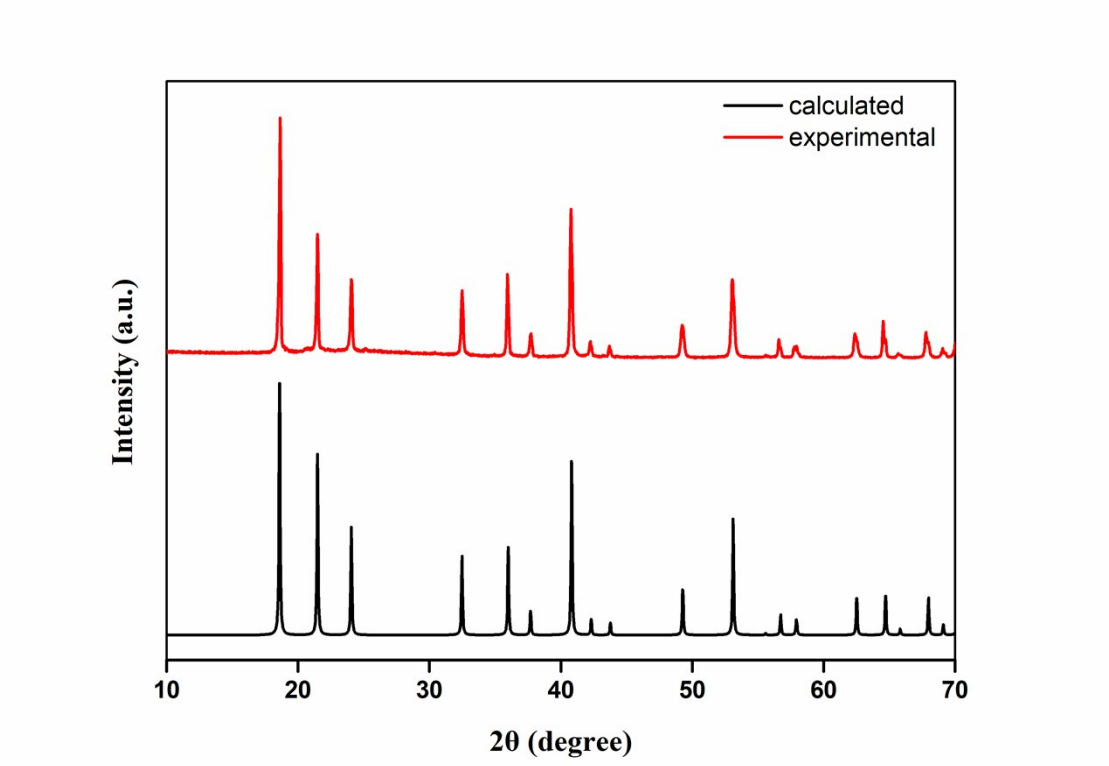

Figure S3. The calculated and experimental powder XRD patterns of Li_2GeTeO_6.

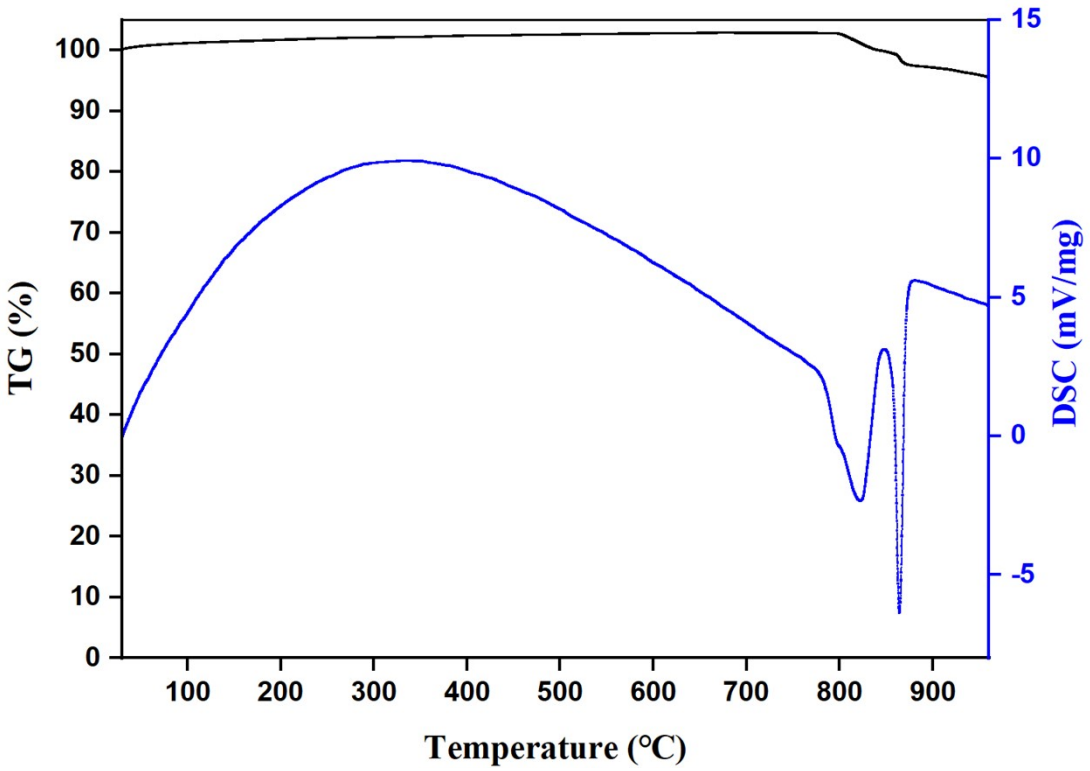

Figure S4. The TG and DSC curves of Li_2GeTeO_6.

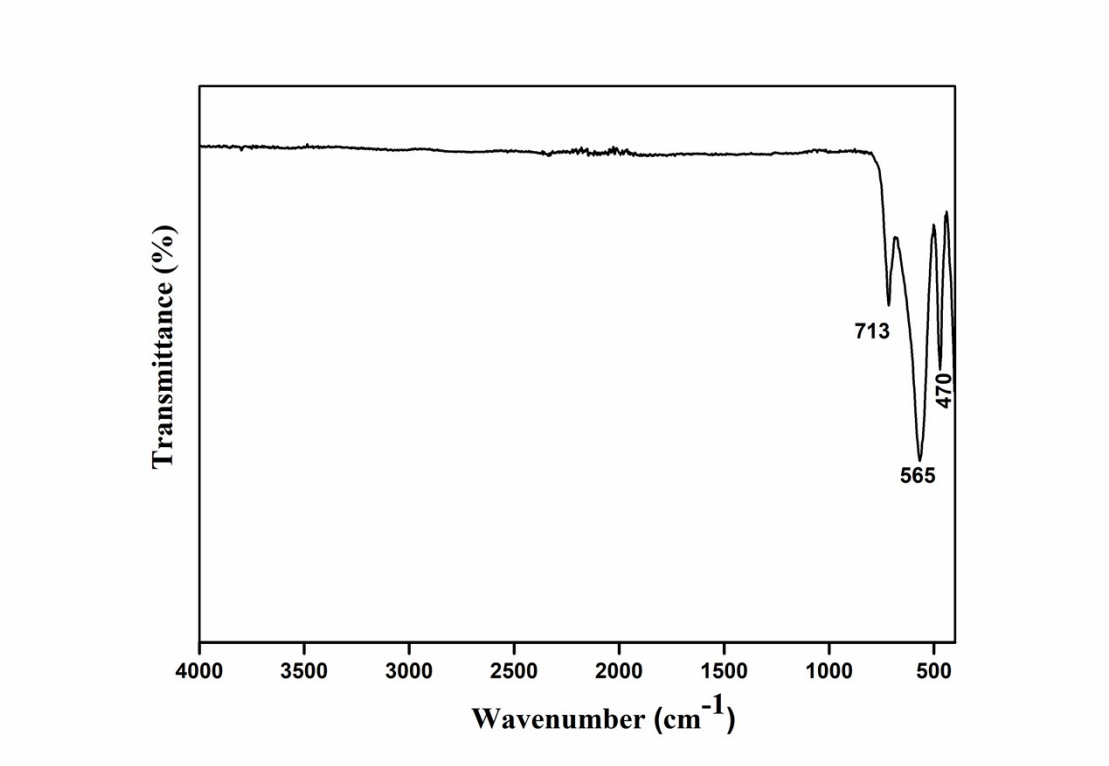

Figure S5. The IR spectrum of Li_2GeTeO_6.

.

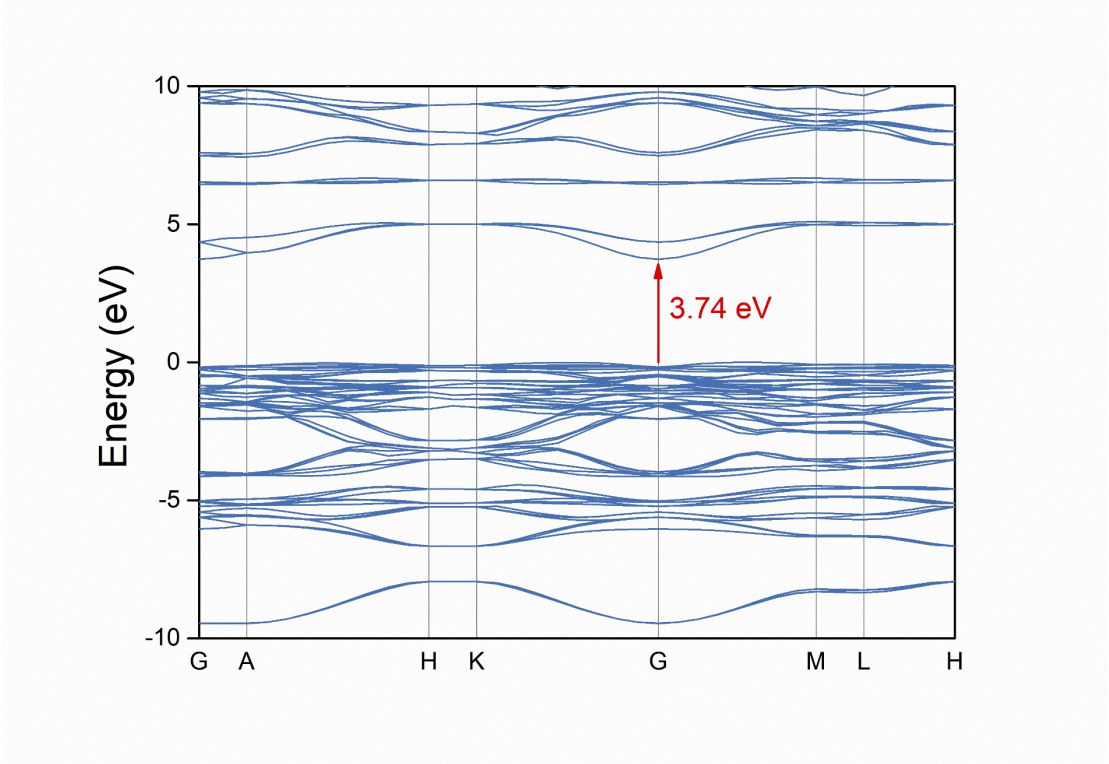

Figure S6. The band gap of Li_2GeTeO_6.

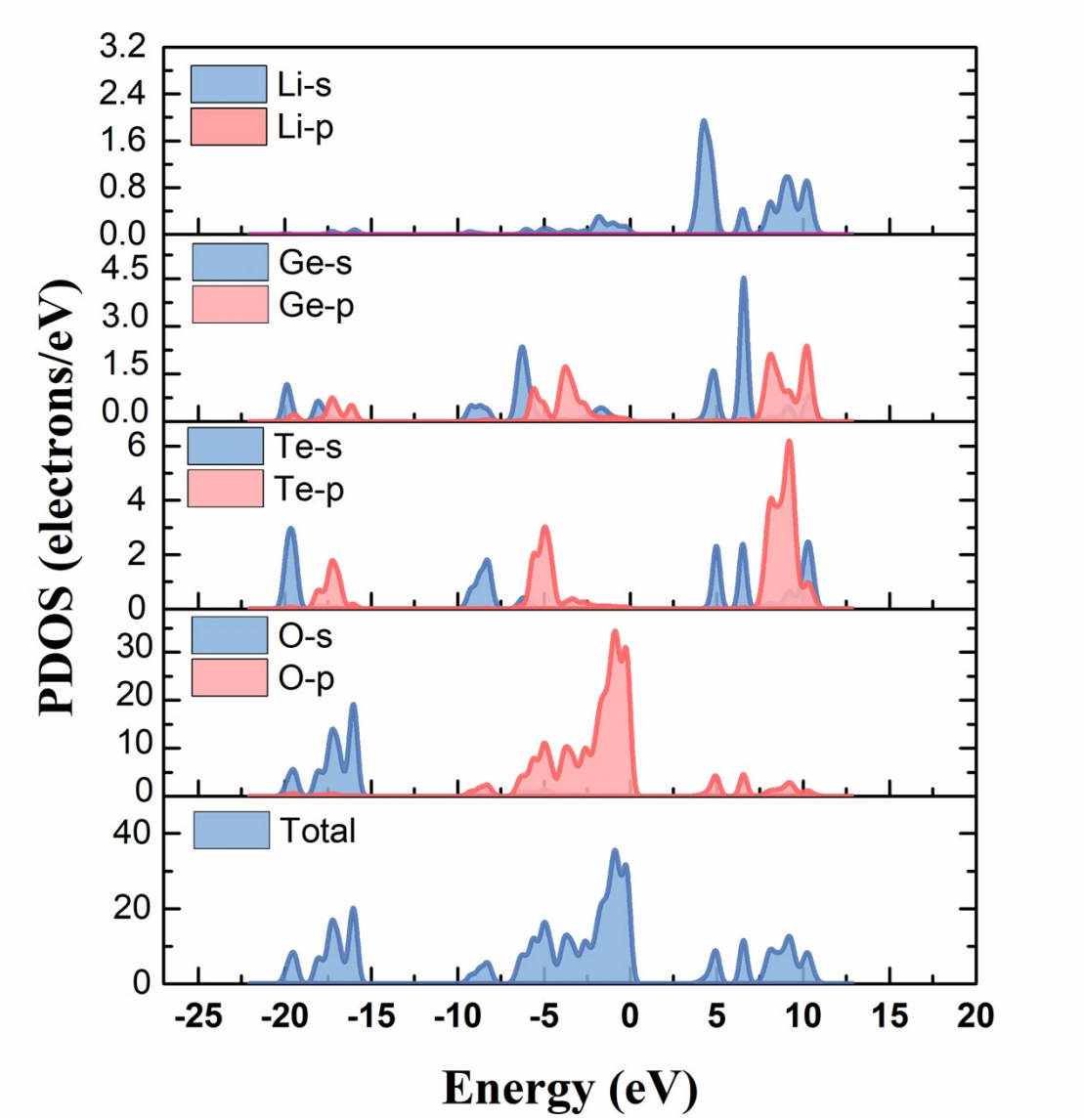

Figure S7. The DOS and PDOS of Li_2GeTeO_6.

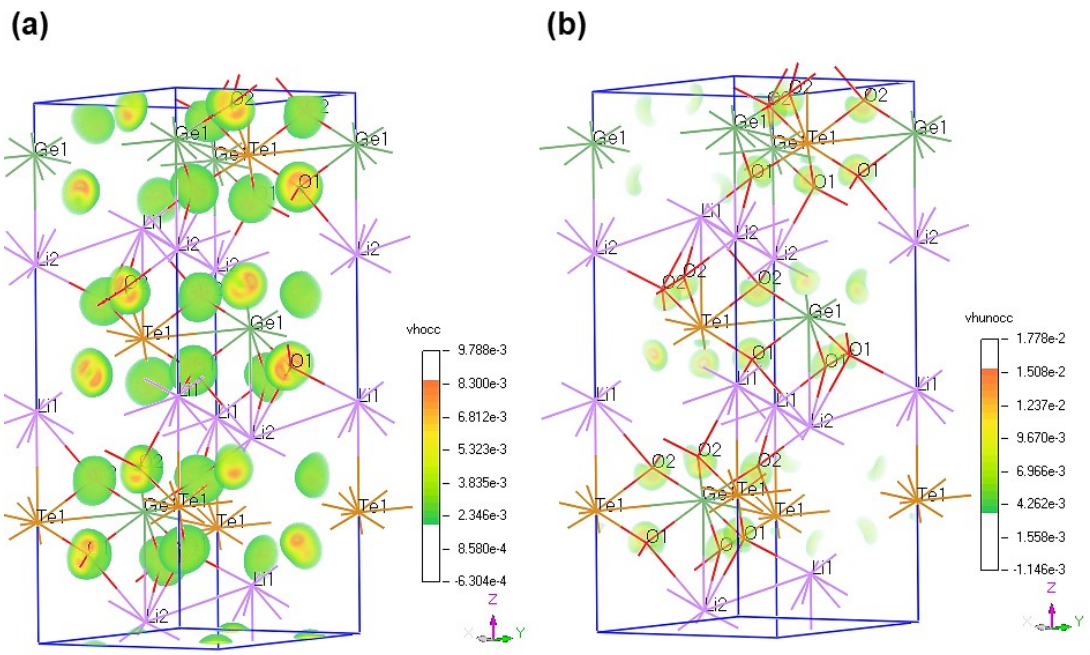

Figure S8. SHG density maps of the occupied and unoccupied orbitals in the VH process of Li_2GeTeO_6. (a) VH occupied; (b)VH unoccupied.

Reference

1. SAINT, *Version 7.60A, Bruker analytical X-ray Instruments, inc.,Madison, WI, 2008*.
2. L. Krause, R. Herbst-Irmer, G. M. Sheldrick and D. Stalke, *J. Appl. Cryst.*, 2015, **48**, 3-10.
3. G. Sheldrick, *Acta Cryst.*, 2015, **A71**, 3-8.
4. G. Sheldrick, *Acta Cryst.*, 2015, **C71**, 3-8.
5. O. V. Dolomanov, L. J. Bourhis, R. J. Gildea, J. A. K. Howard and H. Puschmann, *J. Appl. Cryst.*, 2009, **42**, 339-341.
6. A. L. Spek, *J. Appl. Crystallogr.*, 2003, **36**, 7-13.
7. S. K. Kurtz and T. T. Perry, *J. Appl. Phys.*, 1968, **39**, 3798-3813.
8. S. J. Clark, M. D. Segall, C. J. Pickard, P. J. Hasnip, M. I. J. Probert, K. Refson and M. C. Payne, *Z. Kristallogr.*, 2005, **220**, 567-570.
9. J. S. Lin, A. Qteish, M. C. Payne and V. Heine, *Phys. Rev. B*, 1993, **47**, 4174-4180.
10. A. M. Rappe, K. M. Rabe, E. Kaxiras and J. D. Joannopoulos, *Phys. Rev. B*, 1990, **41**, 1227-1230.
11. S. N. Rashkeev., W. R. L. Lambrecht. and B. Segall., *Phys. Rev. B*, 1998, **57**, 3905-3919.
12. H. K. Liu, Y. Wang, B. B. Zhang, Z. H. Yang and S. L. Pan, *Chem. Sci.*, 2019, **11**, 694-698.
13. M. H. Lee, C. H. Yang and J. H. Jan, *Phys. Rev. B*, 2004, **70**, 235110.